

Loss of Acinus Inhibits Oligonucleosomal DNA Fragmentation but Not Chromatin Condensation during Apoptosis*

Received for publication, September 7, 2005, and in revised form, March 13, 2006. Published, JBC Papers in Press, March 14, 2006, DOI 10.1074/jbc.M509859200

Alvin P. Joselin, Klaus Schulze-Osthoff, and Christian Schwerk¹

From the Institute of Molecular Medicine, the University of Düsseldorf, 40225 Düsseldorf, Germany

Chromatin condensation and oligonucleosomal DNA fragmentation are the nuclear hallmarks of apoptosis. A proteolytic fragment of the apoptotic chromatin condensation inducer in the nucleus (Acinus), which is generated by caspase cleavage, has been implicated in mediating apoptotic chromatin condensation prior to DNA fragmentation. Acinus is also involved in mRNA splicing and a component of the apoptosis and splicing-associated protein (ASAP) complex. To study the role of Acinus for apoptotic nuclear alterations, we generated stable cell lines in which Acinus isoforms were knocked down by inducible and reversible RNA interference. We show that Acinus is not required for nuclear localization and interaction of the other ASAP subunits SAP18 and RNPS1; however, knockdown of Acinus leads to a reduction in cell growth. Most strikingly, down-regulation of Acinus did not inhibit apoptotic chromatin condensation either in intact cells or in a cell-free system. In contrast, although apoptosis proceeds rapidly, analysis of nuclear DNA from apoptotic Acinus knockdown cells shows inhibition of oligonucleosomal DNA fragmentation. Our results therefore suggest that Acinus is not involved in DNA condensation but rather point to a contribution of Acinus in internucleosomal DNA cleavage during programmed cell death.

Activation of a family of cysteinyl aspartate-specific proteases, called caspases, is central to the cellular process of apoptosis or programmed cell death (1, 2). Activated caspases execute cell death via cleavage of specific target proteins, which results in characteristic cytoplasmic and nuclear morphological alterations (3). Whereas cytoplasmic changes include cell shrinkage and membrane blebbing, cleavage of the nuclear lamina, oligonucleosomal laddering of DNA, and condensation of chromatin are the typical nuclear alterations of apoptosis (4, 5).

Several proteins have been described to participate in nuclear changes during cell death (6, 7). One major factor involved in the apoptotic oligonucleosomal fragmentation of nuclear DNA is the caspase-activated DNase (CAD),² which in healthy cells exists as a dimer bound to its inhibitor, ICAD (8, 9). During apoptosis ICAD is cleaved by active

caspase-3 leading to release and activation of CAD. Activated CAD cleaves nuclear DNA at the boundaries between nucleosomes and produces the oligonucleosomal DNA ladder characteristic for apoptotic cells (10, 11). DNA fragmentation by CAD has been also implicated in apoptotic chromatin condensation, because in many cases elimination of CAD activity impairs condensation of chromatin (12–14). Because chromatin condensation at the nuclear periphery can still be observed in the absence of CAD activity, additional factors involved in apoptotic chromatin condensation have been proposed (13, 14). Other mediators involved in apoptotic DNA degradation include the apoptosis-inducing factor (AIF) and endonuclease G (7, 15–18). AIF, which after induction of cell death translocates from the mitochondria to the nucleus, might be responsible for peripheral chromatin condensation in apoptotic cells lacking CAD activity (19).

Another target protein of caspases during apoptosis implicated in nuclear changes is the apoptotic chromatin condensation inducer in the nucleus (Acinus) (20). Acinus is expressed in different isoforms, which are most likely generated by alternative splicing. During apoptosis Acinus is cleaved by caspase-3 and a still unknown protease to produce a 23-kDa fragment (p23) that is contained in all described nonapoptotic isoforms of Acinus. Importantly, Acinus-p23 has been reported to mediate apoptotic chromatin condensation prior to DNA fragmentation in an *in vitro* system utilizing permeabilized cells (20). Cleavage of Acinus might also be involved in nonapoptotic functions of caspases, e.g. during terminal erythroid differentiation, consistent with a potential role in enucleation during erythropoiesis (21, 22).

In subsequent experiments Acinus was identified as a component of functional spliceosomes and as a subunit of a novel apoptosis and splicing-associated protein (ASAP) complex (23–25). In addition to Acinus, the ASAP complex is composed of RNPS1, a general activator of RNA splicing, and SAP18, which has been originally identified as part of the Sin3-histone deacetylase complex (23, 26, 27). Recently, ASAP has also been identified as part of the exon junction complex, a multiprotein complex that is deposited at exon-exon junctions during RNA splicing (28). Thus, these findings suggest that Acinus might be involved in both apoptosis and pre-mRNA processing, which are not necessarily exclusive. Accordingly, Acinus is located in nuclear compartments, termed interchromatin granule clusters, which are thought to function as storage sites for splicing factors (29).

To address the role of Acinus during apoptosis in more detail, we report here the consequences of down-regulation of the nonapoptotic isoforms of Acinus employing an inducible RNA interference (RNAi) system. Knockdown of Acinus causes a slow growth phenotype in HeLa cells. However, depletion of Acinus did not inhibit apoptotic chromatin condensation *in vivo* as well as *in vitro*. Interestingly, although activation of caspases and cleavage of substrates proceeded rapidly, oligonucleosomal DNA fragmentation was inhibited in the Acinus knockdown cells. Our results point to a physiologically significant contribution of

* This work was supported by Grants SFB 503 and SFB 575 from the Deutsche Krebshilfe and the Deutsche Forschungsgemeinschaft. The costs of publication of this article were defrayed in part by the payment of page charges. This article must therefore be hereby marked "advertisement" in accordance with 18 U.S.C. Section 1734 solely to indicate this fact.

¹ To whom correspondence should be addressed: Institute of Molecular Medicine, University of Düsseldorf, Bldg. 23.12, Universitätsstrasse 1, 40225 Düsseldorf, Germany. Tel.: 49-211-81-15975; Fax: 49-211-81-15982; E-mail: Christian.Schwerk@uni-duesseldorf.de.

² The abbreviations used are: CAD, caspase-activated DNase; ICAD, inhibitor CAD; ASAP, apoptosis and splicing-associated protein; LDH, lactate dehydrogenase; DTT, dithiothreitol; PBS, phosphate-buffered saline; PFGE, pulsed-field gel electrophoresis; RT, reverse transcription; DAPI, 4,6-diamidino-2-phenylindole; CHAPS, 3-[(3-cholamidopropyl)dimethylammonio]-1-propanesulfonic acid; PARP, poly(ADP-ribose) polymerase; RNAi, RNA interference; AIF, apoptosis-inducing factor.

Acinus and Apoptosis

Acinus to the activity of apoptotic nucleases or their access to DNA during apoptosis.

MATERIALS AND METHODS

Plasmid Construction—A 19-nucleotide oligonucleotide targeted against nucleotides 3121–3140 of the Acinus mRNA (5'-GAGGCCT-TCTGGATTGACA-3') was designed using the workstation software from OligoEngine (Seattle, WA). The 64-nucleotide short hairpin RNA sense primer 5'-GATCCCCGAGGCCTTCTGGATTGACATTCAA-GAGATGTCAATCCAGAAGGCCTCTTTTGGAAA-3' and the antisense primer 5'-AGCTTTTCCAAAAGAGGCCTTCTGGATTGACATCTCTTGAATGTCAATCCAGAAGGCCTCGGG-3' were annealed and ligated into the pSUPERIOR vector (OligoEngine) according to the manufacturer's instructions.

Tissue Culture, Transfection, and Biological Reagents—HeLa T-REx cells stably expressing the tetracycline repressor were obtained from Invitrogen. Cells were maintained in Dulbecco's modified Eagle's medium with high glucose, supplemented with 10% tetracycline-reduced fetal bovine serum, 100 units/ml penicillin, 0.1 mg/ml streptomycin (all from PAA Laboratories GmbH, Pasching, Austria), and 5 μ g/ml blasticidin (Invitrogen). Cells were transfected using FuGENE 6 reagent (Roche Diagnostics) according to the manufacturer's instructions. 24 h after transfection, the transfected cells were selected using geneticin (G418 solution; PAA Laboratories GmbH).

Staurosporine was obtained from Sigma, and recombinant human TNF- α with a specific activity of 4×10^7 units/mg was from Knoll AG (Ludwigshafen, Germany). Monoclonal antibodies against Mcl-1 and PARP were purchased from Pharmingen and those against c-FLIP were from Alexis Biochemicals (Lausen, Switzerland). An antibody against RNPS-1 (27) was a gift from Akila Mayeda. The antibody against Acinus has been described before (23). Goat antibodies recognizing caspase-3 were obtained from R & D Systems (Wiesbaden, Germany). Rabbit antibodies against SAP18 and ICAD were purchased from Santa Cruz Biotechnology (Santa Cruz, CA). The antibody against phospho-H2A.X (Ser-139) was obtained from Upstate Biotechnology, Inc. (Lake Placid, NY).

Knockdown of Acinus and Survival Assay—Knockdown of Acinus in the HeLa-A3121 stable cell lines was induced by addition of 1 μ g/ml tetracycline (Invitrogen). Cells transfected with the empty pSUPERIOR vector control were treated similarly. Maximal RNA interference and knockdown of Acinus in the A3121 cells were observed after 4–5 days of tetracycline treatment. For experimental analysis, A3121 and pSUPERIOR cells were maintained in tetracycline for 72 h or extended periods. For measurement of cell numbers, cells were either counted or 1×10^4 cells were seeded into 96-well plates in triplicate and were serially diluted 1:1. After 8 days cells were stained with 0.5% crystal violet and 20% methanol for 20 min and washed extensively. Stained cells were solubilized with 33% acetic acid, and the absorbance was measured at 560 nm.

Cell viability after staurosporine treatment was determined by measurement of the release of lactate dehydrogenase (LDH) employing a cytotoxicity detection kit following the instructions of the manufacturer (Roche Diagnostics).

Immunoprecipitations—Extracts for immunoprecipitation were prepared as follows: 1×10^7 cells were collected, and the cell pellets were resuspended in a buffer containing 10 mM HEPES, pH 7.9, 5 mM MgCl₂, 0.25 M sucrose, 10 mM β -mercaptoethanol, and complete protease inhibitor mixture (Roche Diagnostics). Nonidet P-40 was added to a final concentration of 0.1%, and the cells were lysed by freezing and thawing followed by incubation on ice for 10 min. The supernatant or

cytosolic fraction was collected after centrifugation in a microcentrifuge at 14,000 rpm for 5 min at 4 °C. The pellet was dissolved in a buffer containing 10 mM HEPES, pH 7.9, 25% glycerol, 1.5 mM MgCl₂, 0.1 mM EDTA, 10 mM β -mercaptoethanol, and complete protease inhibitor mixture. NaCl was added to a final concentration of 400 mM, and the sample was incubated on ice for 30 min. The sample was freeze-thawed, centrifuged at 14,000 rpm for 15 min at 4 °C, and the supernatants used as input material for immunoprecipitations.

SAP18 antibodies were bound to 10 μ l of protein G-Sepharose beads (Amersham Biosciences) equilibrated in buffer C (20 mM Tris-HCl, pH 7.9, 0.25 mM EDTA, 10% glycerol, 0.5 mM DTT, and 0.2 mM phenylmethylsulfonyl fluoride) containing 100 mM KCl. The beads were incubated for 12 h with 100 μ l of the input material at 4 °C. Following four washes with buffer C containing 500 mM KCl, 0.5 mM DTT, 0.2 mM phenylmethylsulfonyl fluoride, and 0.05% Nonidet P-40, protein complexes were eluted from the beads with 2 \times SDS sample buffer and analyzed by SDS-PAGE and Western blotting.

Cell Extracts, Western Blotting, and Caspase Assays—Cells were washed in phosphate-buffered saline (PBS) and lysed in a high salt buffer containing 1% Nonidet P-40, 20 mM HEPES, pH 7.9, 350 mM NaCl, 20% glycerol, 1 mM MgCl₂, 0.5 mM EDTA, 0.1 mM EGTA, and complete protease inhibitor mixture. The protein content was determined, and equal amounts of proteins were subsequently separated under reducing conditions by SDS-PAGE (4–15% gradient gels) and blotted onto a polyvinylidene difluoride membrane (Amersham Biosciences). Membranes were blocked for 1 h with 5% nonfat dry milk in Tris-buffered saline with 0.05% Tween 20 and then immunoblotted overnight at 4 °C using the respective primary antibody.

Caspase-3 activity in apoptotic cells was determined by incubating cell lysates with 50 μ M of a fluorogenic substrate *N*-acetyl-Asp-Glu-Val-Asp-aminomethylcoumarin (Bachem, Heidelberg, Germany) in 200 μ l of buffer containing 50 mM HEPES, pH 7.3, 100 mM NaCl, 10% sucrose, 0.1% CHAPS, and 10 mM DTT. The release of aminomethylcoumarin was measured by fluorometry using an excitation wavelength of 360 nm and an emission wavelength of 475 nm.

RT-PCR—Total cellular RNA was extracted from 6×10^5 cells using the RNeasy mini kit (Qiagen GmbH, Hilden, Germany). The amount of total RNA was spectrophotometrically determined. 1 μ g of RNA was reverse-transcribed and amplified in a one-step reaction using the TITANIUM One-step RT-PCR kit (Pharmingen) according to the manufacturer's instructions. For amplification of Acinus, primers targeting the following sequences at the C-terminal end of Acinus-L (product size, 326 bp) were used: forward primer 5'-CAGATCGTTTCAGAA-GAGG-3' and reverse primer 5'-CGGGGTGGGCGCCGC-3'. For the amplification of the housekeeping gene glyceraldehyde-3-phosphate dehydrogenase (product size, 329 bp), the following primer pair was used: forward primer 5'-GTGGAAGGACTCATGACCACAG-3' and reverse primer 5'-CTGGTGCTCAGTGTAGCCAG-3'.

DNA Laddering Assays—DNA for detection of apoptotic oligonucleosomal DNA fragmentation was prepared according to the protocol of Hirt (30). Briefly, 2×10^6 cells seeded in 60-mm dishes were washed with PBS and lysed in 1 ml of lysing solution containing 0.5% SDS, 0.1 M NaCl, 5 mM EDTA, 10 mM Tris-HCl, pH 8.0, and 0.1 mg/ml proteinase K, followed by incubation at 37 °C for 2 h. NaCl was added to a final concentration of 1 M, and after overnight incubation at 4 °C, the precipitated salt and SDS were pelleted at 25,000 rpm for 20 min in an ultracentrifuge. The supernatant was extracted with phenol/chloroform, and the DNA was precipitated with ethanol. DNA laddering was then analyzed on 1% agarose gels.

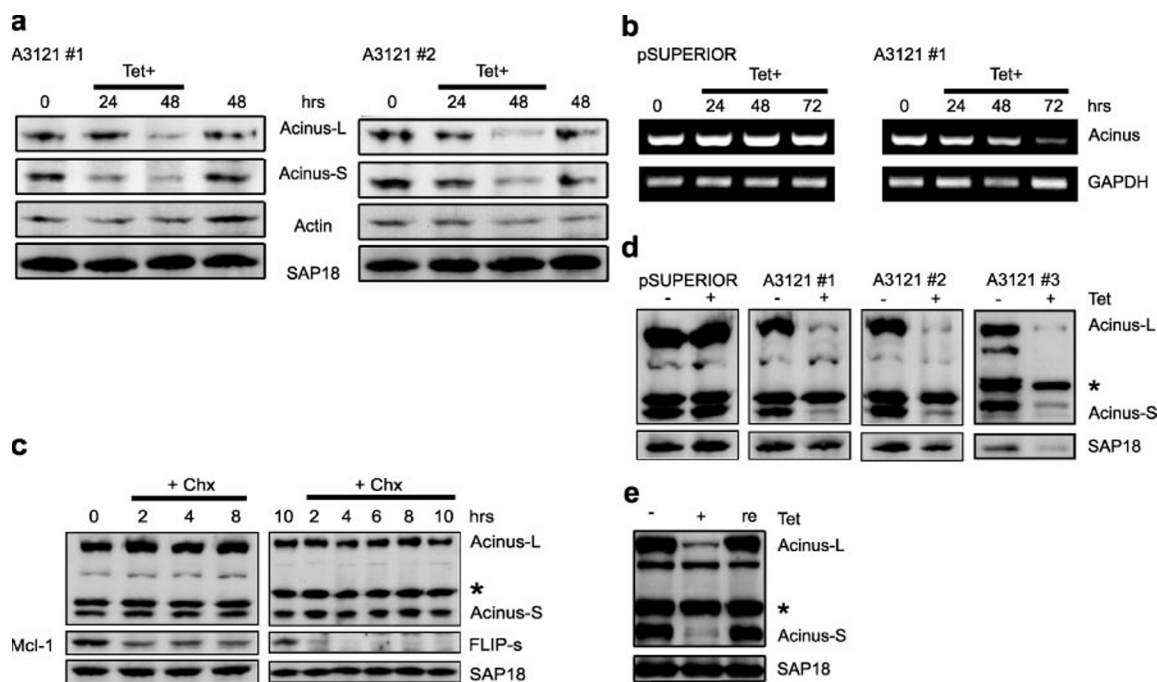


FIGURE 1. A stable, inducible, and reversible knockdown of Acinus in mammalian cells. *a*, time course of Acinus expression after tetracycline (*Tet*) treatment of two Acinus knockdown (HeLa-A3121) clones. HeLa cell clones were treated with tetracycline for 0, 24, and 48 h. Subsequently, whole cell lysates were analyzed for the presence of both Acinus isoforms, SAP18 and β -actin. As a control, extracts of noninduced cells were analyzed after 48 h. *b*, RT-PCR analysis of Acinus knockdown cells. HeLa-pSUPERIOR control cells and HeLa-A3121 cells (clone 1) were induced for RNAi with tetracycline for the indicated periods of time. Acinus transcripts were detected by RT-PCR. Glyceraldehyde-3-phosphate dehydrogenase (*GAPDH*) transcripts were analyzed as control. *c*, analysis of the turnover rate of the ASAP components Acinus and SAP18. HeLa cells were incubated in the presence of cycloheximide (*Chx*) for the indicated time. Subsequently, whole cell extracts were analyzed for the presence of the indicated proteins by Western blotting. Although the apoptosis inhibitors Mcl-1 and FLIP-s demonstrated a fast protein turnover rate, the amounts of both Acinus isoforms and SAP18 remained virtually unchanged. An unspecific protein detected by the Acinus antibody is indicated by an asterisk. *d*, long term tetracycline treatment of HeLa-pSUPERIOR cells and three independent HeLa-A3121 clones. HeLa cells were treated with tetracycline for 8 days and subsequently examined for the presence of the indicated proteins by Western blot analysis. Noninduced cells were analyzed as control. An unspecific protein detected by the Acinus antibody is indicated by an asterisk. *e*, the Acinus knockdown is reversible. HeLa-A3121 cells were released from tetracycline treatment and grown for several days. Extracts from cells either untreated (–), induced for knockdown (+), or released from knockdown (*re*) were analyzed by Western blot.

Pulsed-field Gel Electrophoresis (PFGE)—Plugs for PFGE were prepared using the CHEF mammalian genomic DNA plug kit (Bio-Rad) according to the manufacturer's instructions. PFGE was performed using the Gene Path System (Bio-Rad). 1% certified megabase-agarose (Bio-Rad) horizontal gels were run at 14 °C with program no. 18 for the separation of 50 kb to 1 Mb DNA fragments for 19.5 h.

In Vitro Chromatin Condensation Assays—Cyttoplasmic extracts for *in vitro* chromatin condensation assays were prepared as described (31) with slight alterations. Briefly, cells were washed with PBS and harvested by scraping from the tissue culture dishes. After one more wash with PBS, cells were suspended with cold buffer B (50 mM HEPES, pH 7.5, 110 mM potassium acetate, 2 mM magnesium acetate, 2 mM EGTA) and resuspended in 1.5 volume of buffer A (50 mM HEPES, pH 7.5, 10 mM potassium acetate, 2 mM magnesium acetate, 2 mM EGTA) containing 2 mM DTT and protease inhibitor mixture. After swelling on ice for 30 min, the cells were lysed by douncing. Subsequently, nuclei and cell debris were spun down at $1500 \times g$ for 10 min. The supernatant was spun again at $100,000 \times g$ for 30 min. In the final supernatant the potassium acetate concentration was adjusted to 110 mM. For permeabilization, cells were rinsed twice with buffer B and then treated with buffer B containing 2 mM DTT, 20 $\mu\text{g}/\text{ml}$ digitonin, and 1 $\mu\text{g}/\text{ml}$ DAPI for 45 min at room temperature, followed by two washing steps with buffer B containing 2 mM DTT.

For *in vitro* chromatin condensation assays 25 μl of reaction mixture was added to the permeabilized cells and sealed with a coverslip. The reaction mixture contained 300 μg of cytoplasmic extract, 5 μM phosphocreatine, 20 units/ml creatine kinase, 1 mM ATP and, where indicated, 1 μg of recombinant caspase-3. Control reactions were performed in the absence of cytoplasmic extract. The reactions were

incubated for 3 h at 37 °C and analyzed using an Axiovert135 microscope (Zeiss, Germany) equipped with OpenLab software (Improvision, Tübingen, Germany).

RESULTS

Stable Vector-mediated, Inducible, and Reversible Knockdown of Acinus—To achieve an inducible knockdown of Acinus, we stably transfected HeLa T-REx cells with a tetracycline-regulated pSUPERIOR RNAi construct (A3121), which was directed against a sequence contained in all described isoforms of Acinus. As experimental control, the empty pSUPERIOR plasmid was stably introduced into HeLa T-REx cells. After selection of cells with stable integration of the plasmids, individual clones were analyzed for down-regulation of Acinus. Significant knockdown of both the long and short isoform of Acinus was detected in three individual clones on the level of protein (Fig. 1*a*) as well as RNA (Fig. 1*b*) after 48–72 h of induction of RNA interference with tetracycline when compared with a control clone containing only the empty vector. The three clones exhibited comparable results in all analyses presented below.

Because the reduction of target proteins in RNAi experiments is directly related to protein turnover rates, we examined the stability of Acinus by treatment of cells with cycloheximide. As can be seen in Fig. 1*c*, Acinus as well as the ASAP subunit SAP18 displayed a rather slow turnover rate when compared with the Bcl-2 protein Mcl-1 or the caspase-8 inhibitor FLIP-s. Thus, maximal reduction of Acinus requires induction of RNAi over a longer period of time. This was confirmed by examination of three independent long term tetracycline-treated Acinus knockdown clones, which allowed reduction of Acinus isoforms to >95% (Fig. 1*d*). We reproducibly observed that also in absence of tetra-

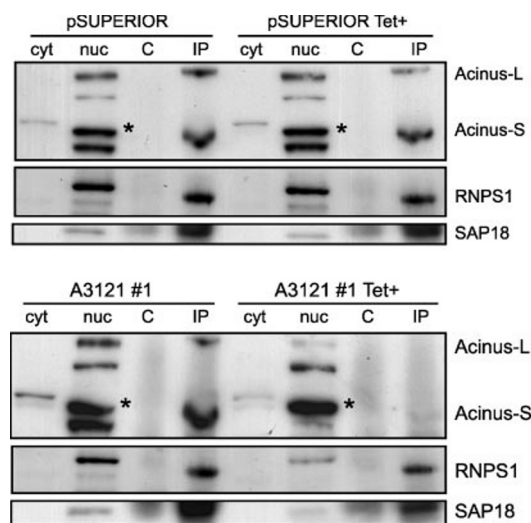


FIGURE 2. Acinus isoforms are not required for complex formation and nuclear localization of SAP18 and RNPS1. Nuclear (*nuc*) and cytoplasmic (*cyt*) extracts were prepared from HeLa-pSUPERIOR and HeLa-A3121 cells (clone 1) grown in the absence or presence (*Tet*+) of tetracycline. Antibodies against SAP18 (*IP*) but not empty control beads (*C*) co-immunoprecipitate RNPS1 and Acinus isoforms. The presence of SAP18, RNPS1, and Acinus isoforms in the cellular fractions and IP eluates was examined by Western blot analysis. An unspecific protein detected by the Acinus antibody is indicated by an asterisk. The slightly different mobility of the proteins in the lysates and immunoprecipitation reactions is because of different salt concentrations.

cycline the amounts of Acinus in HeLa-A3121 cells were lower compared with the control cells, indicating that some background RNAi occurred even in noninduced cells (Fig. 1*d* and data not shown). Additionally, it is noteworthy that knockdown of Acinus led to a slight but reproducible reduction of SAP18, an interaction partner of Acinus, in all three clones (Fig. 1*d*). Reduction of subunits of a multiprotein complex after knockdown of another subunit has been described before (32). Knockdown of Acinus was reversible, because removal of tetracycline restored Acinus expression (Fig. 1*e*).

Subsequently experiments were performed with long term tetracycline-treated cells to achieve a maximum reduction of Acinus isoforms. Additionally, cells induced for RNAi against Acinus for 72 h were used to demonstrate that results obtained with the knockdown cells are not because of secondary effects caused by long term depletion of Acinus.

Acinus Is Not Required for Maintaining a Nuclear SAP18-RNPS1 Complex—Nuclear ASAP complexes are composed of the subunits SAP18, RNPS1, and distinct Acinus isoforms (23). To examine whether depletion of Acinus influences the cellular localization of the other ASAP subunits as well as the interaction between RNPS1 and SAP18, we generated cytoplasmic and nuclear fractions from HeLa-pSUPERIOR and HeLa-A3121 cells cultured in the absence and presence of tetracycline. Western blot analysis showed that components of the ASAP complex are exclusively detectable in the nuclear fraction under all conditions investigated, indicating that Acinus is not required for nuclear localization of SAP18 and RNPS1 (Fig. 2). To determine whether an interaction between SAP18 and RNPS1 is maintained in the absence of Acinus, we performed immunoprecipitation experiments employing an antibody directed against SAP18. Significantly, although comparable amounts of RNPS1 were co-immunoprecipitated with SAP18 under all conditions, virtually no Acinus isoforms could be detected by Western blotting in the eluates from the immunoprecipitations (Fig. 2). Similar results were obtained with HeLa-A3121 cells induced with tetracycline for 72 h, although due to less complete knockdown small amounts of Acinus isoforms co-immunoprecipitated with SAP18 (data not shown). These results implicate that an interaction between SAP18 and RNPS1 persists after depletion of Acinus isoforms.

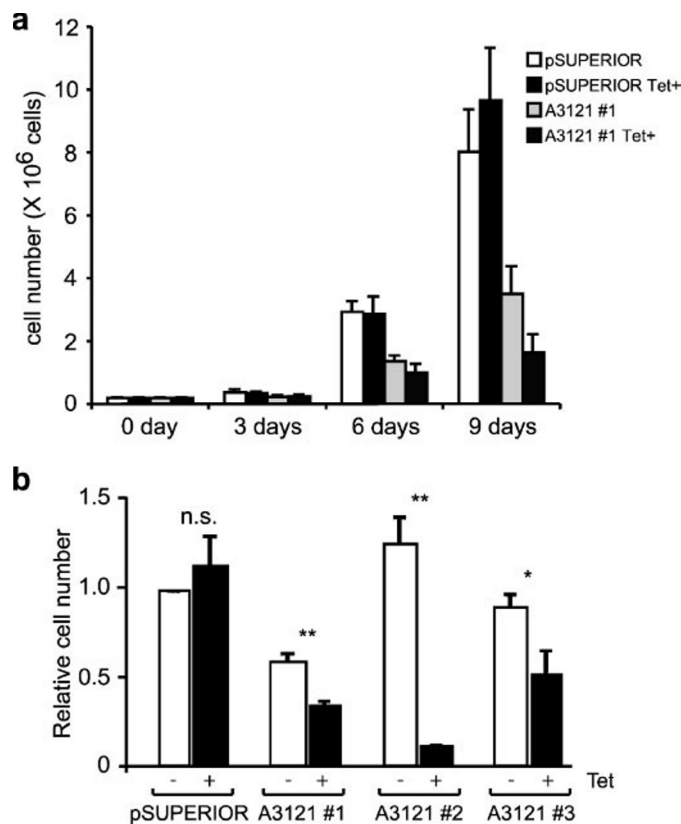


FIGURE 3. Knockdown of Acinus causes a slow growth phenotype. *a*, growth characteristics for HeLa-pSUPERIOR and HeLa-A3121 (clone 1). Cells were cultured in the presence or absence of tetracycline (*Tet*) for 9 days and counted every 3 days. The bar diagram shows the average values \pm S.D. of two independent experiments. *b*, serial dilutions were performed for HeLa-pSUPERIOR as well as HeLa-A3121 cells, which had been cultured in the presence (*Tet*+) or absence of tetracycline. Appropriate wells were stained with crystal violet after 8 days, and cell growth was evaluated by densitometric analysis. The bar diagram shows the average values \pm S.D. from three independent experiments with HeLa-pSUPERIOR cells and three HeLa-A3121 clones. The cell number of untreated HeLa-pSUPERIOR cells was set as 1. *n.s.*, not significant; *, $p < 0.05$; **, $p < 0.01$; *t* test for related samples.

Induction of Acinus Knockdown Leads to a Slow Growth Phenotype—One of the first observations when analyzing the RNAi clones was a clear reduction of cell growth after induction of Acinus knockdown by treatment of HeLa-A3121 cells with tetracycline. The growth characteristics of HeLa-A3121 cells cultured in the presence and absence of tetracycline compared with HeLa-pSUPERIOR cells are shown in Fig. 3*a*. To allow a quantification of cell growth, we performed serial dilutions of three independent Acinus knockdown clones as well as pSUPERIOR control cells in the presence and absence of tetracycline. An evaluation of cell growth after crystal violet staining and subsequent densitometric analysis is shown in Fig. 3*b*. Addition of tetracycline caused a significant reduction of cell growth in three independent HeLa-A3121 clones, but not in HeLa-pSUPERIOR control cells. Noteworthy, the reduced cell growth of the Acinus knockdown cells was not because of induction of cellular senescence, as determined by a senescence-associated β -galactosidase assay (data not shown).

Caspase Activation and Substrate Cleavage Proceed Rapidly in Acinus Knockdown Cells—In its original description Acinus had been identified as a factor involved in nuclear apoptotic processes (20). To analyze whether knockdown of Acinus has a general influence on the progress of apoptosis, we produced whole cell extracts from HeLa-pSUPERIOR and HeLa-A3121 cells grown in the presence or absence of tetracycline. The cells had been treated with the apoptosis inducer staurosporine for different amounts of time. Because a hallmark of apoptosis is the acti-

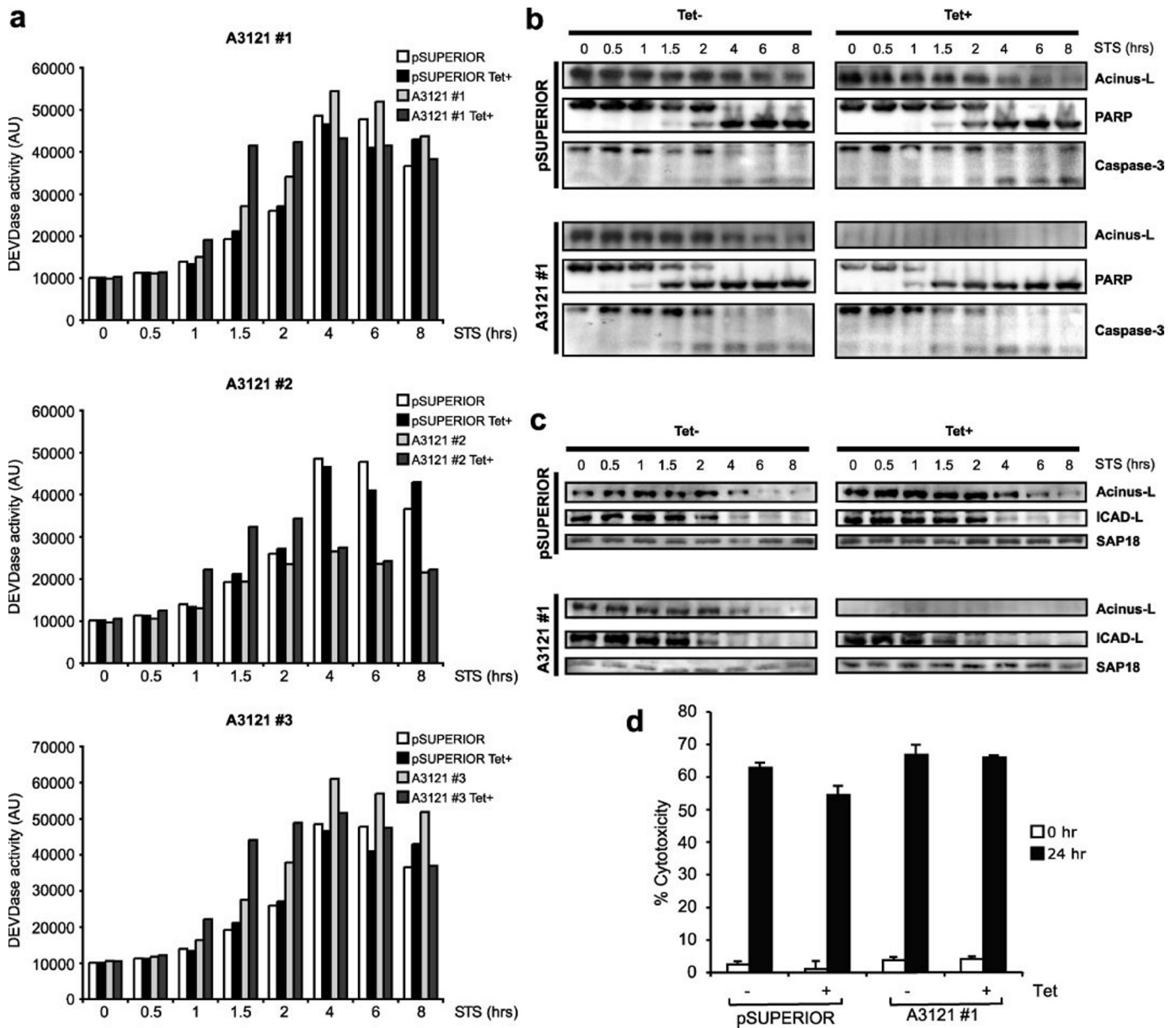


FIGURE 4. Activation of caspases and cleavage of substrates in apoptotic Acinus knockdown cells. HeLa-pSUPERIOR cells as well as three independent HeLa-A3121 clones were grown in the presence (*Tet*⁺) or absence of tetracycline and induced for cell death with the kinase inhibitor staurosporine (STS). Cell extracts were analyzed for markers of apoptosis at the indicated time points. *a*, measurement of caspase-3-like activity. Caspase-3-like proteases are activated rapidly in Acinus knockdown cells. *b* and *c*, analysis of substrate cleavage in apoptotic HeLa-pSUPERIOR and HeLa-A3121 cells. Cleavage of the caspase substrates PARP (*b*) and ICAD (*c*) as well as caspase-3 processing in cells treated with STS for the indicated time was investigated by Western blotting with the antibodies indicated at the right. Cleavage of PARP and ICAD correlates with activation of caspases in Acinus knockdown cells. *d*, LDH release from HeLa-pSUPERIOR and HeLa-A3121 cells (not induced or induced for RNAi for 4 days) treated with 1 μ M staurosporine for 24 h. Measurements were performed in triplicate. Shown is the percentage of release compared with the maximum possible release. Cytotoxicity was determined by the release of LDH into supernatants and calculated as percentage of total cellular LDH activity.

vation of caspases, we employed a substrate assay to determine caspase-3-like activity in the cell extracts. As can be seen in Fig. 4*a*, caspase-3-like proteases were rapidly activated in Acinus knockdown cells with substrate cleavage clearly detectable already after 1.5 h of staurosporine treatment. A close inspection of the progress of substrate cleavage indicated that even a slight acceleration of caspase activation might have occurred.

We next investigated whether activation of caspases was accompanied by cleavage of target proteins in Acinus knock-down cells. Analysis of the caspase substrates PARP (Fig. 4*b*) and ICAD (Fig. 4*c*) by Western blotting confirmed cleavage during the progress of apoptosis, which paralleled the activation of caspases seen in the substrate assay, again indicating a slight acceleration of cell death might have occurred in

Acinus knockdown cells. For instance, whereas only partial PARP cleavage was detectable in the control or noninduced HeLa-A3121 cells 2 h after staurosporine treatment, Acinus knockdown cells revealed complete PARP cleavage already after 1.5 h of treatment, accompanied by significant loss of the full-length form of ICAD. Significant lactate dehydrogenase release was detected after 24 h (Fig. 4*d*), showing that the cells died after incubation with staurosporine.

Apoptotic Chromatin Condensation Is Not Inhibited by Depletion of Acinus—Condensation of nuclear chromatin is a phenomenon observed late during apoptosis following activation of caspases and cleavage of substrates. Because Acinus had been implicated to function in apoptotic chromatin condensation (20), we analyzed the progress of chromatin condensation during apoptosis in Acinus knockdown cells.

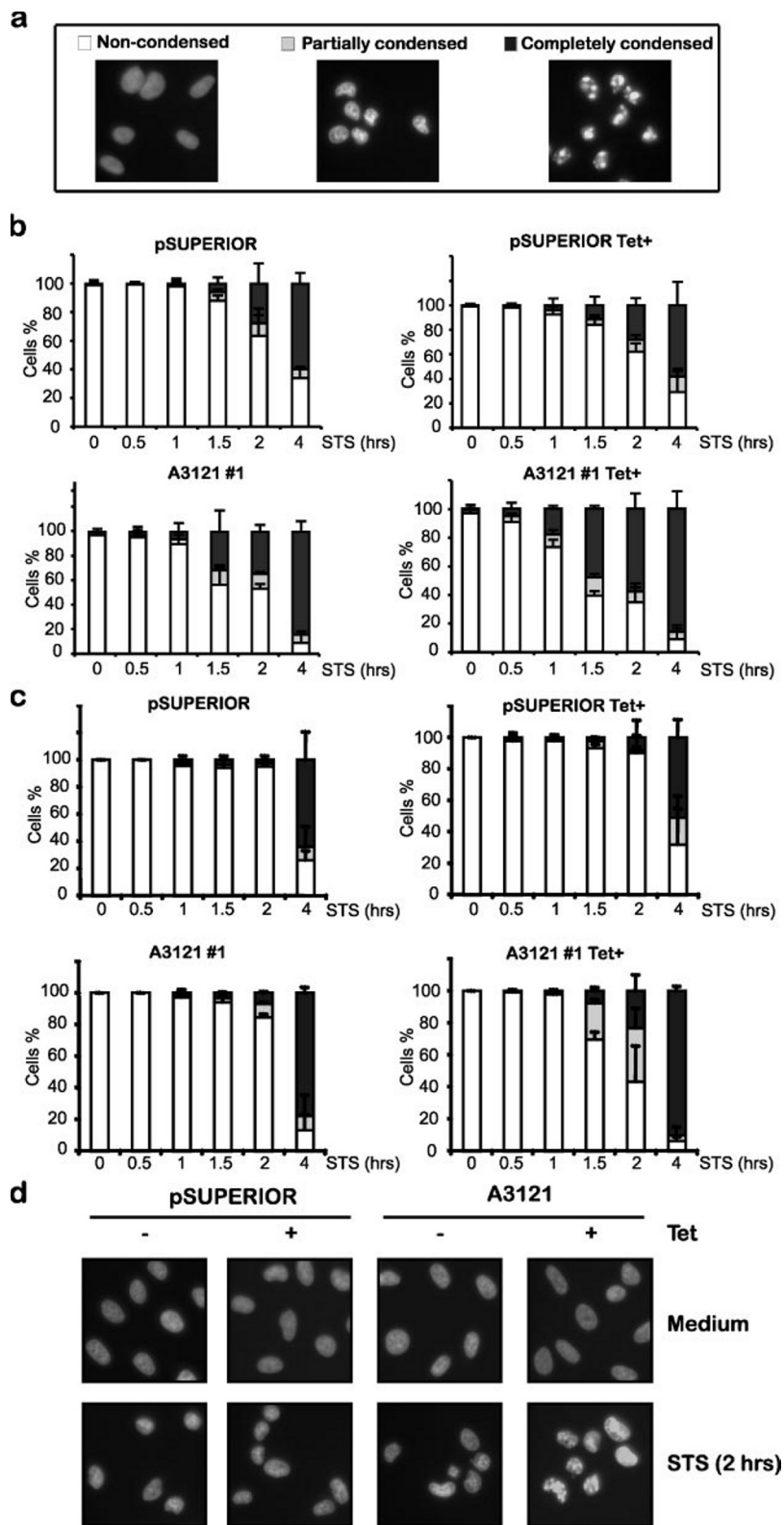


FIGURE 5. Apoptotic chromatin condensation in Acinus knockdown cells. *a*, tetracycline-treated (*Tet*⁺) or untreated HeLa-pSUPERIOR and HeLa-A3121 cells were induced to undergo apoptosis with 1 μ M staurosporine (STS) for the indicated time and then stained with DAPI. Stained nuclei were visualized by fluorescence microscopy. Nuclei were classified as noncondensed, partially condensed, or completely condensed. Cells with partially condensed chromatin display beginning of chromatin condensation at the nuclear periphery, whereas in cells with complete chromatin condensation the chromatin masses separate from each other into discrete clumps. *b*, quantitative analysis of apoptotic chromatin condensation. HeLa-pSUPERIOR and HeLa-A3121 cells had been cultured in the presence of tetracycline for 72 h. Results show the mean values \pm S.D. from triplicates with an average of 150 nuclei counted per condition. *c*, same as in *b*, except long term treated cells were used. Results show the mean values \pm S.D. from quadruplicates with 200 nuclei counted per condition. *d*, fluorescence microscopic visualization of apoptotic chromatin condensation in long term treated cells.

For that purpose HeLa-pSUPERIOR and HeLa-A3121 cells were treated with staurosporine. After different incubation times, the level of apoptotic chromatin condensation was determined by DAPI staining and scored in three sequential stages (noncondensed, partially condensed, and completely condensed chromatin; Fig. 5*a*). As can be seen in Fig. 5, depletion of Acinus by RNAi did not inhibit condensation of chromatin

after induction of apoptosis but did rather cause a slight acceleration of chromatin condensation, possibly related to earlier activation of caspases. This effect could be observed in cells induced for knockdown for 72 h (Fig. 5*b*) as well as in long term induced cells (Fig. 5*c*). Titration of staurosporine from 0.25 to 1 μ M revealed a similarly accelerated condensation of chromatin in the Acinus-depleted cells under all con-

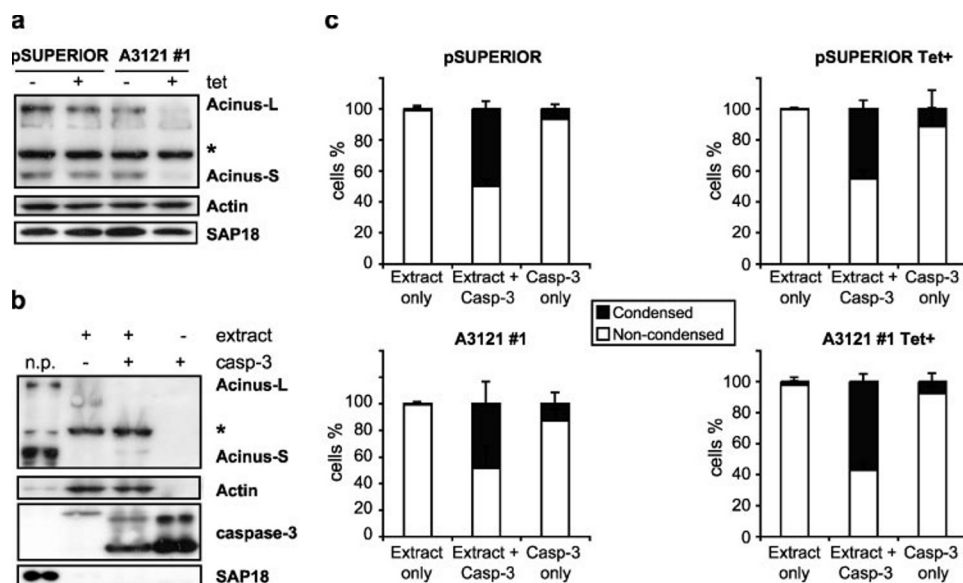


FIGURE 6. Induction of apoptotic chromatin condensation in a cell-free *in vitro* system depleted of Acinus for 72 h. *a* and *b*, Western blot analyses of cellular extracts employed in the *in vitro* chromatin condensation assay. *a*, whole cell extracts were prepared from HeLa-pSUPERIOR and HeLa-A3121 cells grown in the presence or absence of tetracycline (*tet*) for 72 h and analyzed with the antibodies indicated at the right. *b*, cytoplasmic extracts were prepared from HeLa cells and added to *in vitro* chromatin condensation assays where indicated. Also, recombinant caspase-3 (*casp-3*) was added to some of the reactions. The reaction mixtures were analyzed by Western blotting with the antibodies indicated at the right. A nuclear pellet (*n.p.*) fraction from HeLa cells was loaded as control. *c*, *in vitro* chromatin condensation assay employing permeabilized HeLa-pSUPERIOR and HeLa-A3121 cells grown in the absence and presence (*Tet*+) of tetracycline. Cytoplasmic extracts were added to the permeabilized cells in the presence or absence of recombinant active caspase-3. Control reactions were performed in the presence of caspase-3 only. After incubation for 3 h DAPI-stained nuclei were analyzed by fluorescence microscopy. Nuclei were classified as noncondensed or condensed. Results show the mean values \pm S.D. of triplicates with an average of 300 nuclei counted per condition.

ditions investigated, although apoptosis was delayed at lower staurosporine concentrations (data not shown). Furthermore, we did not observe inhibition of chromatin condensation in Acinus knockdown cells employing tumor necrosis factor α plus cycloheximide as apoptotic stimulus (data not shown). pSUPERIOR control cells grown in the absence and presence of tetracycline exhibited identical apoptotic chromatin condensation under all conditions analyzed.

Acinus has been reported to be required for apoptotic chromatin condensation in a cell-free system using permeabilized nuclei (20). Because we did not observe an inhibition of apoptotic chromatin condensation in HeLa-A3121 cells after tetracycline treatment (Fig. 5), we employed a cell-free system to analyze the influence of the Acinus knockdown on chromatin condensation *in vitro*. For these experiments HeLa-A3121 cells containing Acinus or depleted of Acinus by treatment with tetracycline for 72 h (Fig. 6) or by long term treatment (Fig. 7), respectively, as well as HeLa-pSUPERIOR control cells were used. After permeabilization with digitonin, chromatin condensation reactions were initiated by addition of a cytoplasmic HeLa cell extract devoid of Acinus isoforms in the presence and absence of recombinant active caspase-3. Control reactions were performed with recombinant caspase-3 alone. The efficiency of the Acinus knockdown in the digitonin-permeabilized cells (Figs. 6*a* and 7*a*) as well as the absence of Acinus in the cytoplasmic extracts (Figs. 6*b* and 7*b*) were controlled by Western blotting. As can be seen in Figs. 6*c* and 7*c*, significant apoptotic chromatin condensation was detectable in the permeabilized cells only when both the cytoplasmic extract and active caspase-3 were added. However, regardless of the presence or absence of Acinus, comparable levels of chromatin condensation could be observed under all conditions (Fig. 6*c* and 7*c*). Thus, both *in vivo* and *in vitro* chromatin condensation is not affected by depletion of Acinus.

Acinus Knockdown Inhibits Apoptotic DNA Fragmentation—Oligonucleosomal laddering of nuclear DNA during cell death is caused by CAD (7, 10, 11). To analyze involvement of Acinus in apoptotic DNA fragmentation, we prepared DNA from HeLa-A3121 cells grown in the

presence and absence of tetracycline, which had been treated with staurosporine for different amounts of time. Surprisingly, as can be seen in Fig. 8, *a* and *b*, oligonucleosomal DNA fragmentation was impaired in HeLa-A3121 cells when knockdown of Acinus was caused by tetracycline treatment. In contrast, HeLa-A3121 cells expressing Acinus as well as HeLa-pSUPERIOR control cells, which were either grown in absence or presence of tetracycline, showed no inhibition of DNA fragmentation during cell death.

Additionally to oligonucleosomal DNA laddering by activated CAD, apoptotic DNA fragmentation displays high molecular weight cleavage potentially involving further nucleases, *e.g.* AIF and endonuclease G (7, 15–18). To examine whether high molecular weight cleavage still occurs in the Acinus knockdown cells, we separated DNA prepared from HeLa A3121 cells grown in the presence and absence of tetracycline by pulsed-field gel electrophoresis. As can be seen in Fig. 9*a*, high molecular weight DNA fragments above 50 kb comparable with uninduced HeLa-A3121 or pSUPERIOR control cells still occurred in cells depleted for Acinus after treatment with staurosporine.

Phosphorylation of the histone variant H2A.X at serine 139 is a marker for the appearance of DNA double strand breaks during apoptosis. Appearance of H2A.X phosphorylation coincides with the generation of high molecular weight DNA fragments (33). To investigate whether H2A.X phosphorylation still occurs in the Acinus knockdown cells after induction of apoptosis, extracts from cells grown in the presence and absence of tetracycline were analyzed by Western blotting with an antibody recognizing H2A.X phosphorylated at serine 139. As can be seen in Fig. 9*b*, similar amounts of H2A.X phosphorylation could be detected after induction of apoptosis under all conditions analyzed, confirming that DNA double strand breaks still occur in the Acinus-depleted cells. Consistent with the results obtained in Acinus knockdown cells, phosphorylation of H2A.X was also observed in MCF7 breast carcinoma cells (data not shown), which are devoid of oligonucleosomal DNA fragmentation during apoptosis due to lack of caspase-3 activity (34).

FIGURE 7. Induction of apoptotic chromatin condensation in a cell-free *in vitro* system employing extracts from cells depleted long term for Acinus. *a* and *b*, Western blot analyses of cellular extracts employed in the *in vitro* chromatin condensation assay were performed as in Fig. 6. *c*, *in vitro* chromatin condensation assay employing permeabilized HeLa-pSUPERIOR and HeLa-A3121 cells grown in the absence and presence (*Tet*+) of tetracycline were performed as in Fig. 6. After incubation for 3 h, DAPI-stained nuclei were analyzed by fluorescence microscopy and photographed. *n.p.*, nuclear pellet; *casp-3*, caspase-3.

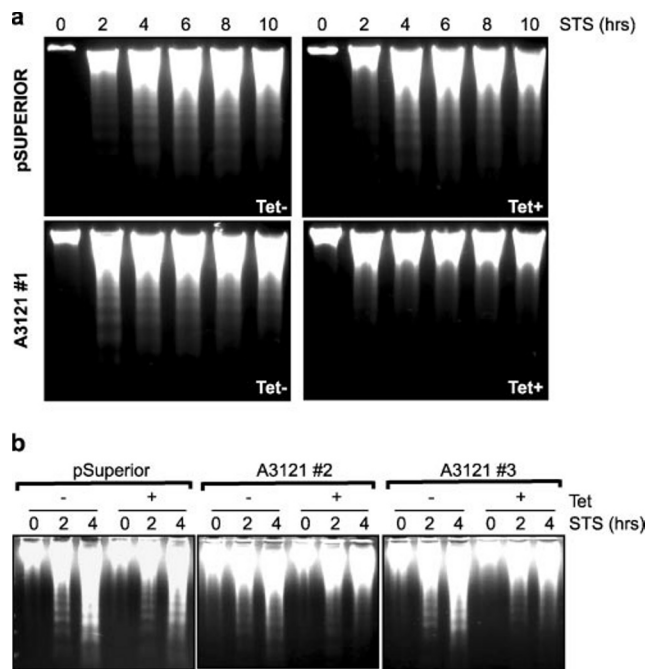
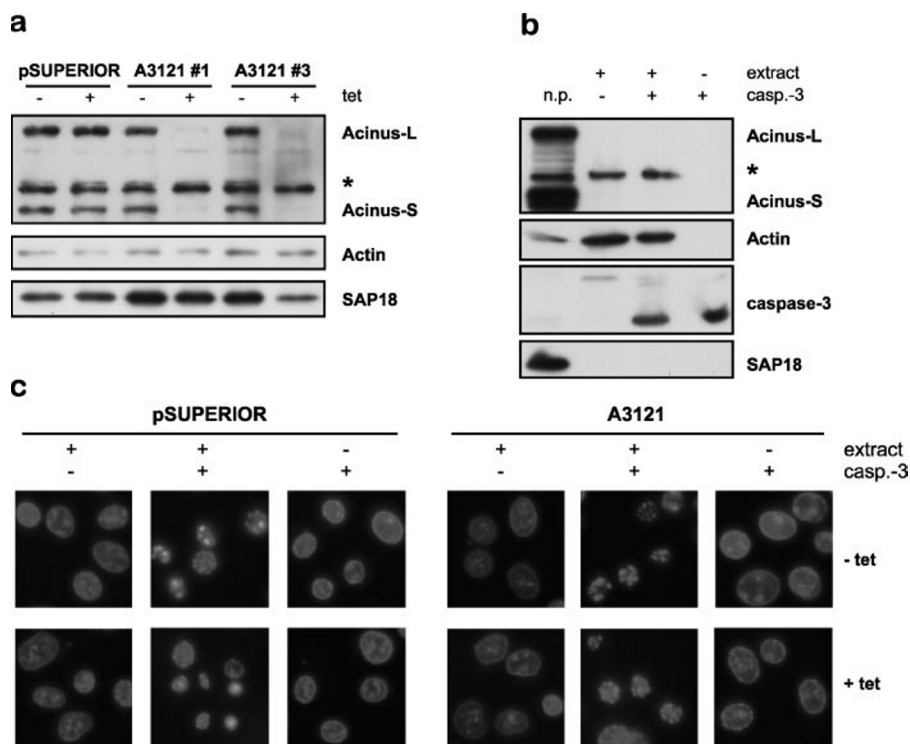


FIGURE 8. Oligonucleosomal DNA fragmentation is inhibited in apoptotic Acinus knockdown cells. HeLa-pSUPERIOR and HeLa-A3121 cells grown in the absence or presence (*Tet*+) of tetracycline were treated with staurosporine (STS) for the indicated periods of time. Subsequently, DNA was prepared as described under "Materials and Methods" and separated on a 1% agarose gel. HeLa-A3121 cells (*a*, clone 1; *b*, clones 2 and 3) depleted for Acinus demonstrate an inhibition of apoptotic oligonucleosomal DNA fragmentation.

DISCUSSION

Fragmentation and condensation of nuclear DNA are hallmarks of apoptotic cell death. The nuclear protein Acinus, which is a target of caspases during apoptosis, had been proposed previously as an important factor involved in apoptotic chromatin condensation (20). We have employed an inducible RNA interference approach to further analyze

functions of Acinus during programmed cell death. By using this method we were able to achieve very efficient depletion of Acinus isoforms to an extent of >95% after induction of RNAi with tetracycline, a process that was completely reversible.

During analysis of the Acinus knockdown clones, it was obvious that the cells displayed a reduced growth rate when Acinus was depleted. This effect was not because of an increase in senescence (data not shown). Because Acinus is involved in apoptotic processes, we analyzed the response of Acinus knockdown cells to apoptotic stimuli. Different markers of cell death, including activation of caspases and cleavage of the caspase substrates PARP and ICAD, showed that cells depleted for Acinus proceed rapidly into cell death. A close inspection of the progress of apoptosis indicated that a slight acceleration of cell death might have occurred in the Acinus knockdown cells, suggesting that the decreased growth rate of Acinus-depleted cells is caused by a higher background rate of spontaneous apoptosis.

Concomitant with caspase activation and substrate cleavage Acinus knockdown cells exhibited normal or even higher levels of apoptotic condensation of chromatin *in vivo*. We could confirm this result in a cell-free system employing active recombinant caspase-3 and a cell extract, which was devoid of detectable Acinus. This result was surprising, because a 23-kDa fragment of Acinus (p23), which is produced during apoptosis, has been shown to be required for apoptotic chromatin condensation in an *in vitro* assay (20). Furthermore, in that study antisense-mediated depletion of Acinus has been reported to effectively delay DNA condensation. Additionally, in a recent study reduction of chromatin condensation was observed in an Acinus knockdown system (35). Although we cannot rule out that trace amounts of Acinus left in the knockdown cells were sufficient to mediate condensation of chromatin, we believe that Acinus is not required for chromatin condensation during apoptosis in our system. We could not observe reduction of chromatin condensation despite the fact that Acinus was virtually completely depleted in our experimental system. The reason for the discrepancy to the published data (20, 35) is currently unknown, but it might be due to different experimental setups and/or cell types. It is also conceiv-

able that inhibition of apoptotic chromatin condensation described in some *in vivo* systems reflects impairment of DNA fragmentation that we observe in the Acinus knockdown cells. It should be also noted that a more recent study (36) reported that caspase-6-mediated cleavage of lamin A is essential for chromatin condensation.

Two different pathways are thought to mediate nuclear DNA fragmentation and condensation during apoptosis (19). In one pathway, leading to condensation of chromatin at the nuclear periphery, the DNA is cleaved into high molecular weight fragments of about 50–300 kb. Nucleases or cofactors, which are proposed to be involved in this pathway, include AIF and endonuclease G, topoisomerase II, and cyclophilins (7). Internucleosomal cleavage of DNA additionally to large scale DNA fragmentation occurs in the second pathway. This process can be visualized on agarose gels as an oligonucleosomal DNA ladder, which is typical for cells undergoing apoptosis. Executive in this pathway is CAD, which is activated after cleavage of its inhibitor, ICAD. Although the mechanisms of high molecular weight DNA fragmentation are less established, the two pathways may function in parallel, but presumably mostly occur in a stepwise fashion (19).

Importantly, we observed an impairment of oligonucleosomal DNA fragmentation in the Acinus knockdown cells, which is most likely due to inhibition of the nucleolytic activity of CAD. The observed inhibition of oligonucleosomal DNA fragmentation is not caused by a reduction of apoptosis, because the progress of apoptosis (including activation of caspases and cleavage of substrates) was not inhibited in Acinus knockdown cells.

DNA double strand breaks still occurred after induction of cell death as detected by the appearance of high molecular weight DNA fragmentation and concomitant H2A.X phosphorylation. This observation is in agreement with the detection of apoptotic chromatin condensation in the knockdown cells. It is possible that depletion of Acinus impairs CAD activity by interfering with the access of CAD to the nuclear DNA. Also, DNA binding of the CAD-ICAD complex prior to induction of cell death has been shown to stimulate the activity of CAD after cleavage of ICAD (37). Alternatively, Acinus might directly influence CAD activity. Along this line, biochemical experiments have suggested that interactions with other nuclear proteins, including histone H1, high mobility group proteins 1/2, and topoisomerase II, may regulate the nuclease activity of CAD (38–40). Experiments employing a CAD-GFP fusion protein have proposed that upon induction of caspase-3-dependent apoptosis activated CAD associates with a subnuclear compartment defined as the nuclear matrix (41). Noteworthy, DNA at nuclear matrix regions is most exposed and A/T-rich, and CAD displays a preference for A/T-rich DNA regions (reviewed in Ref. 10). Interestingly, the long isoform of Acinus (Acinus-L) contains at its N terminus a SAP domain, which constitutes a proposed DNA-binding domain with preference for A/T-rich sequences (42, 43). It is therefore possible that depletion of Acinus by knockdown interferes with cleavage of nuclear DNA at A/T-rich regions prior to degradation of the DNA into nucleosomal units.

The observation that loss of Acinus leads to an inhibition of DNA fragmentation, whereas caspases are rapidly activated, seems contradictory at first view. However, there are several possibilities that could explain this finding. We have shown previously that Acinus is a subunit of an ASAP complex (23). This is in line with the localization of Acinus in functional spliceosomes (24, 25) as well as the presence of ASAP in the exon junction complex (28) and implicates a function of Acinus in splicing regulation. It is known that a large number of apoptotic factors is regulated by alternative splicing (44), including the CAD-regulatory factor ICAD, which is expressed in two isoforms with putatively distinct regulatory potential (45). Importantly and in line with our data, a recent

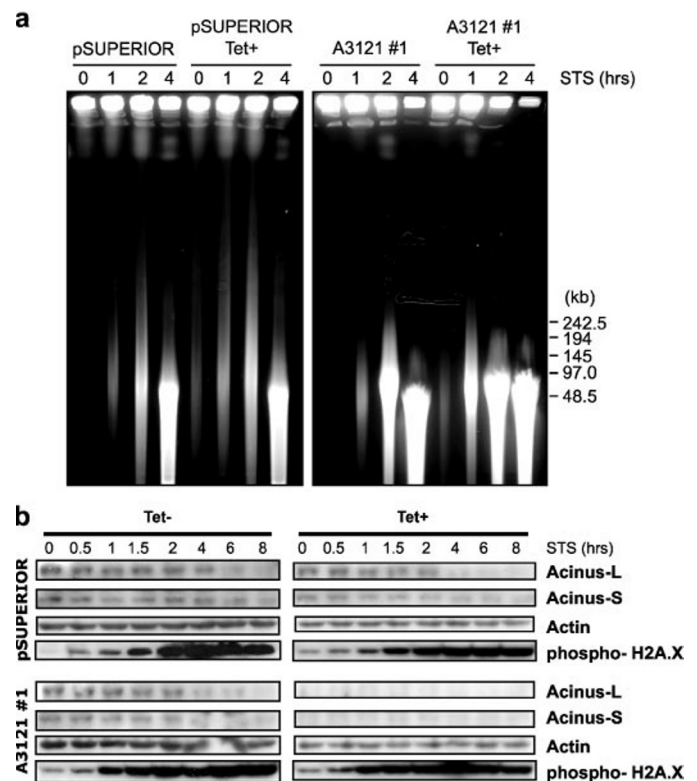


FIGURE 9. High molecular weight DNA cleavage still occurs in apoptotic Acinus knockdown cells. *a*, HeLa-pSUPERIOR and HeLa-A3121 cells grown in the absence or presence of tetracycline (*Tet*⁺) were treated with staurosporine (STS) for the indicated periods of time. Subsequently, DNA was prepared and separated by pulsed-field gel electrophoresis as described under "Materials and Methods." *b*, analysis of H2A.X phosphorylation at serine 139 in HeLa-pSUPERIOR and HeLa-A3121 cells. Cells had been induced for RNAi with tetracycline or left uninduced. Apoptosis was induced with 1 μ M staurosporine, and samples were taken at the indicated time points and analyzed by Western blotting for the proteins indicated at the right.

study demonstrated that loss of the splicing factor ASF/SF2 causes apoptosis despite a concomitant inhibition of oligonucleosomal DNA fragmentation in a chicken cell line (35). Inhibition of DNA fragmentation correlated with a shift in ICAD isoform expression. It is therefore possible that depletion of Acinus also influences the splicing patterns of apoptotic factors involved in DNA degradation during cell death, *e.g.* ICAD. This might involve the splicing-activating function of the ASAP subunit RNPS1 (27), whose presence in the nucleus persists after Acinus knockdown.

Dysfunction of the splicing machinery by gene targeting of splicing factors has been also reported to result in lethality in *Caenorhabditis elegans* (46). In insect cells, genetic inactivation of the SR protein splicing factor ASF/SF2 causes cell death (47). Defects in the splicing machinery result most likely in the activation of a DNA damage-response pathway. Dysfunctional mRNA splicing, for instance by inactivation of ASF/SF2, has been shown to cause DNA double strand breaks and genomic instability because of formation of DNA/RNA hybrid R loop structures, which are formed between nascent transcripts and DNA (48). Thus, in analogy to chemotherapeutic drugs, DNA damage might trigger activation of the mitochondrial death pathway. However, because the exact role of Acinus in RNA splicing regulation is unknown, it is currently unclear whether increased DNA damage is also responsible for the acceleration of caspase activation upon Acinus depletion. In summary, although the exact role of Acinus during apoptotic chromatin condensation remains to be deciphered, we have discovered a novel and unexpected function of Acinus in DNA degradation during programmed cell death.

Acknowledgments—We thank Dr. Akila Mayeda for the antibody against RNPS1, Drs. Grete Berns and Matthias Drechsler for help with pulsed-field gel electrophoresis, and Dr. Axel Schwerk for help with statistical analyses.

REFERENCES

- Los, M., Wesselborg, S., and Schulze-Osthoff, K. (1999) *Immunity* **10**, 629–639
- Strasser, A., O'Connor, L., and Dixit, V. M. (2000) *Annu. Rev. Biochem.* **69**, 217–245
- Fischer, U., Janicke, R. U., and Schulze-Osthoff, K. (2003) *Cell Death Differ.* **10**, 76–100
- Kerr, J. F., Wyllie, A. H., and Currie, A. R. (1972) *Br. J. Cancer* **26**, 239–257
- Wyllie, A. H., Kerr, J. F., and Currie, A. R. (1980) *Int. Rev. Cytol.* **68**, 251–306
- Zamzami, N., and Kroemer, G. (1999) *Nature* **401**, 127–128
- Samejima, K., and Earnshaw, W. C. (2005) *Nat. Rev. Mol. Cell Biol.* **6**, 677–688
- Liu, X., Zou, H., Slaughter, C., and Wang, X. (1997) *Cell* **89**, 175–184
- Enari, M., Sakahira, H., Yokoyama, H., Okawa, K., Iwamatsu, A., and Nagata, S. (1998) *Nature* **391**, 43–50
- Nagata, S., Nagase, H., Kawane, K., Mukae, N., and Fukuyama, H. (2003) *Cell Death Differ.* **10**, 108–116
- Earnshaw, W. C. (1995) *Curr. Opin. Cell Biol.* **7**, 337–343
- Zhang, J., Liu, X., Scherer, D. C., van Kaer, L., Wang, X., and Xu, M. (1998) *Proc. Natl. Acad. Sci. U. S. A.* **95**, 12480–12485
- Sakahira, H., Enari, M., Ohsawa, Y., Uchiyama, Y., and Nagata, S. (1999) *Curr. Biol.* **9**, 543–546
- Samejima, K., Tone, S., and Earnshaw, W. C. (2001) *J. Biol. Chem.* **276**, 45427–45432
- Saelens, X., Festjens, N., Vande Walle, L., van Gurp, M., van Loo, G., and Vandenaebelen, P. (2004) *Oncogene* **23**, 2861–2874
- Li, L. Y., Luo, X., and Wang, X. (2001) *Nature* **412**, 95–99
- Parrish, J., Li, L., Klotz, K., Ledwich, D., Wang, X., and Xue, D. (2001) *Nature* **412**, 90–94
- Susin, S. A., Lorenzo, H. K., Zamzami, N., Marzo, I., Snow, B. E., Brothers, G. M., Mangion, J., Jacotot, E., Costantini, P., Loeffler, M., Larochette, N., Goodlett, D. R., Aebersold, R., Siderovski, D. P., Penninger, J. M., and Kroemer, G. (1999) *Nature* **397**, 441–446
- Susin, S. A., Dugas, E., Ravagnan, L., Samejima, K., Zamzami, N., Loeffler, M., Costantini, P., Ferri, K. F., Irinopoulou, T., Prevost, M. C., Brothers, G., Mak, T. W., Penninger, J., Earnshaw, W. C., and Kroemer, G. (2000) *J. Exp. Med.* **192**, 571–580
- Sahara, S., Aoto, M., Eguchi, Y., Imamoto, N., Yoneda, Y., and Tsujimoto, Y. (1999) *Nature* **401**, 168–173
- Schwerk, C., and Schulze-Osthoff, K. (2003) *Biochem. Pharmacol.* **66**, 1453–1458
- Zermati, Y., Garrido, C., Amsellem, S., Fishelson, S., Bouscary, D., Valensi, F., Varet, B., Solary, E., and Hermine, O. (2001) *J. Exp. Med.* **193**, 247–254
- Schwerk, C., Prasad, J., Degenhardt, K., Erdjument-Bromage, H., White, E., Tempst, P., Kidd, V. J., Manley, J. L., Lahti, J. M., and Reinberg, D. (2003) *Mol. Cell Biol.* **23**, 2981–2990
- Zhou, Z., Licklider, L. J., Gygi, S. P., and Reed, R. (2002) *Nature* **419**, 182–185
- Rappsilber, J., Ryder, U., Lamond, A. I., and Mann, M. (2002) *Genome Res.* **12**, 1231–1245
- Zhang, Y., Iratni, R., Erdjument-Bromage, H., Tempst, P., and Reinberg, D. (1997) *Cell* **89**, 357–364
- Mayeda, A., Badolato, J., Kobayashi, R., Zhang, M. Q., Gardiner, E. M., and Krainer, A. R. (1999) *EMBO J.* **18**, 4560–4570
- Tange, T. O., Shibuya, T., Jurica, M. S., and Moore, M. J. (2005) *RNA (N. Y.)* **11**, 1869–1883
- Saitoh, N., Spahr, C. S., Patterson, S. D., Bubulya, P., Neuwald, A. F., and Spector, D. L. (2004) *Mol. Biol. Cell* **15**, 3876–3890
- Hirt, B. (1967) *J. Mol. Biol.* **26**, 365–369
- Adam, S. A., Marr, R. S., and Gerace, L. (1990) *J. Cell Biol.* **111**, 807–816
- Strack, S., Cribbs, J. T., and Gomez, L. (2004) *J. Biol. Chem.* **279**, 47732–47739
- Rogakou, E. P., Nieves-Neira, W., Boon, C., Pommier, Y., and Bonner, W. M. (2000) *J. Biol. Chem.* **275**, 9390–9395
- Janicke, R. U., Sprengart, M. L., Wati, M. R., and Porter, A. G. (1998) *J. Biol. Chem.* **273**, 9357–9360
- Hu, Y., Yao, J., Liu, Z., Liu, X., Fu, H., and Ye, K. (2005) *EMBO J.* **24**, 3543–3554
- Ruchaud, S., Korfali, N., Villa, P., Kottke, T. J., Dingwall, C., Kaufmann, S. H., and Earnshaw, W. C. (2002) *EMBO J.* **21**, 1967–1977
- Korn, C., Scholz, S. R., Gimadutdinov, O., Lurz, R., Pingoud, A., and Meiss, G. (2005) *J. Biol. Chem.* **280**, 6005–6015
- Liu, X., Li, P., Widlak, P., Zou, H., Luo, X., Garrard, W. T., and Wang, X. (1998) *Proc. Natl. Acad. Sci. U. S. A.* **95**, 8461–8466
- Liu, X., Zou, H., Widlak, P., Garrard, W., and Wang, X. (1999) *J. Biol. Chem.* **274**, 13836–13840
- Durrieu, F., Samejima, K., Fortune, J. M., Kandels-Lewis, S., Osheroff, N., and Earnshaw, W. C. (2000) *Curr. Biol.* **10**, 923–926
- Lechardeur, D., Xu, M., and Lukacs, G. L. (2004) *J. Cell Biol.* **167**, 851–862
- Aravind, L., and Koonin, E. V. (2000) *Trends Biochem. Sci.* **25**, 112–114
- Kipp, M., Gohring, F., Ostendorp, T., van Drunen, C. M., van Driel, R., Przybylski, M., and Fackelmayr, F. O. (2000) *Mol. Cell Biol.* **20**, 7480–7489
- Schwerk, C., and Schulze-Osthoff, K. (2005) *Mol. Cell* **19**, 1–13
- Samejima, K., and Earnshaw, W. C. (2000) *Exp. Cell Res.* **255**, 314–320
- Longman, D., Johnstone, I. L., and Caceres, J. F. (2000) *EMBO J.* **19**, 1625–1637
- Wang, J., Takagaki, Y., and Manley, J. L. (1996) *Genes Dev.* **10**, 2588–2599
- Li, X., and Manley, J. L. (2005) *Cell* **122**, 365–378